Impact of Rotation and Chemical Reactions on MHD Mixed Convection Flow over an Inclined Heated Porous Plate with Heat and Mass Transfer Analysis

R. KAVITHA[1,*], J. ANGEL[2]
[1]Department of Mathematics and Statistics,
Faculty of Science and Humanities, SRM Institute of Science and Technology,
Kattankulathur Campus, Chengulpattu Campus,
INDIA

[2]Department of Mathematics,
Vel tech Rangarajan Dr Sagunthala R&D Institute of Science and Technology,
Avadi,
INDIA

*Corresponding Author

Abstract: - The impact of rotation and chemical reaction are examined concerning the MHD flow of incompressible, viscous, and electrically conducting fluid over an inclined moving heated porous plate. It has been described how mass transfer affects MHD mixed convection flow across an infinite vertical plate. The perturbation approach is utilized to solve the coupled partial differential equations that are non-linear. Graphs have been used to study and analyze the effects of various relevant parameters on concentration profile, temperature, and velocity profile. These parameters include the Schmidt number (Sc), Grashof number (Gr), Prandtl number(Pr), modified Grashof number(Gm), heat source (ϕ), Rotational (R), chemical reaction (γ), magnetic field (M) permeability parameter (K) and angle of inclination (α). An explanation of the linked heat and mass transport processes is given. We noticed that the velocity decreases for rising the value of Rotational R. The findings of the current study are comparison with the outcome obtained by Veeresh C et al. in the presence of Rotational; our results seem to be in useful accord with the data that are already available.

Key-Words: - Chemical reaction, Rotation, Thermal Radiation, MHD, Porous Medium, Perturbation Method, Incompressible Fluid, heat and mass transfer.

1 Introduction

Rotating flow is vital for a variety of scientific, engineering, and product design purposes. The topic offers a way to simulate and consequently, develop things like vacuum cleaners, jet engines, and pumps. The concept of rotation is often essential to comprehending and simulating the particular flow mechanics, even in applications where it is not immediately apparent. The mathematical description of rotating flow can be formulated from the viewpoint of a stationary observer. Since all of the boundary conditions impacting the flow would be described in terms of the rotating frame, it is frequently more straightforward to modify the momentum equation so that they can be applied in a rotating frame of reference. This is particularly true for a variety of rotating machinery, including those with a single rotor that revolves inside stationary casings. In these situations, tracking the flow from a fixed coordinate system to the rotating components is very helpful. There remains a prolonged gap, so in addition to giving the reader observation into customizing regular and particular rotating flow applications, it seeks to describe the topic of rotating flow and related phenomena. For many mathematicians, physicists, and engineers, the topic of rotating fluids is crucial. Rotation and sun radiation work together to regulate the weather system on Earth. The earth's rotation causes the jet wind and ocean circulations; rotation-induced swirl is what gives rise to extreme phenomena like hurricanes and tornadoes. Applications involving circle, and pipe geometries and comparing non-zero

vortex to irrational flow, in which fluid particles flow in straight lines are highlighted.

The fluid flow actions of an electrolyte in the direction of a field of magnets are the subject of magnetohydrodynamics. Several key discoveries about the transfer of heat and mass in MHD are made, including improved heat transfer, control of flow, and linked phenomena. Rotation can affect the MHD's overall results, the flow's uniformity, and capacity to transport heat. Heat transmission in porous media is essential in several domains, such as chemical production, nuclear reaction cooling, MHD generation, geothermal energy extraction, and petroleum engineering. Heat and mass transmission are crucial concepts in many scientific and technical applications; they are involved in heat engines, heat diodes, thermodynamic heating elements, and chemically processed heat exchangers, among other systems. Additionally, mass transfer plays a significant role in procedures like absorption and filtration through membranes. In this three-dimensional setting, this study aims to investigate the characteristics of such flow [1], [2], [3].

In their research, [4] examined the transport of heat through radiation. The evaporation of ethanol is an example of a process where the transfer of mass by air circulation is observed and mass transfer principles are used in a variety of domains including metallurgy, household humidifiers, astrophysics, and geophysics. The radiation effect on the unstable convection-free movement via a titled permeable plate with a heat source was covered by [5]. In the presence of the radiating effect, [6] investigated the independent convection and heat transmission of a Couette flow across an infinitely porous plate.

The heat source flow of MHD between vertically alternate conduction walls with the Hall effect was covered by [7]. The Hall and rotating effects on an unstable MHD rotating circulation for a second-grade flow through a medium when chemical reactions and an associated magnetic field were additionally present were studied by [8]. Because chemical reactions have so many practical uses, such as melting, ceramics, glassware manufacturing, and catalytic reactors, inquiry into heat and mass transfer using these reactions has expanded dramatically. These reactions fall into two categories: heterogeneous, which happens at interfaces or limited places, and homogeneous, which happens throughout the process.

[9] described the potential effects of suction on a homogeneous rotating vertical surface in a chemical reaction. Moreover, research on plasma confinement shows promise in resolving the world's energy crisis, a critical issue facing human society by [10]. The effect of sliding overflow of fluids that are both non-Newtonian and Newtonian was covered by [11]. The effects of homogeneous transverse magnetic fields applied to solid surfaces or fluids have been widely studied in MHD research. For several applications in several disciplines, including weather, solar science, intergalactic fluid dynamics, astronomy, and geophysical sciences.

In industrial settings, magneto-convection plays a particularly important role in processes like controlled fusion research, electromagnetic pumping, crystal growth, MHD bearing, plasma jet operation, and magnetic regulation of melting iron in steel production. It also affects fluid metal refreshing in nuclear reactors. Furthermore, the design and functioning of dependable machinery in the industrial sector, nuclear power stations, turbines for gas, and engine systems for airplanes, missiles, satellites, and spacecraft depend on radiation heat and mass transfer. Gaining an understanding of these connections is essential to developing technologies and enhancing output in these vital domains [12], [13], [14], [15] and [16].

[17] explored the impact of impulsive motion on Eyring-Powell nanofluid flow across a rotating sphere, incorporating MHD and convective regimes with entropy analysis. Their focus on non-Newtonian fluids and the combined effects of magnetic fields and fluid rotation adds depth to current MHD studies, particularly in systems influenced by impulse forces and nanofluid characteristics [18] delve into the mixed convection nanofluid flow over a rotating sphere, highlighting the role of liquid hydrogen and ammonia diffusion. This study examines the interaction between chemical species in mixed convection systems and their influence on nanofluid behavior, offering insights into the design of chemical processes in MHD environments. [19] investigated unsteady MHD flow past an inclined vertical porous plate, accounting for the combined effects of chemical reactions, aligned magnetic fields, radiation, and Soret effects. Their research provides a comprehensive view of how these factors influence heat and mass transfer in MHD systems, making significant contributions to applications involving porous media. [20] explored the role of Lorentz force on non-Newtonian dusty rotating fluid in the presence of tiny particles of dust and TiO2. Their work underscores the importance of nanoparticles in enhancing thermal conductivity and modifying fluid behavior, which is particularly relevant for industrial processes involving dusty environments. [21] analyzed MHD oscillatory Casson fluid flow in the presence of heat absorption, chemical reactions, and

Soret effects. This research contributes to a deeper understanding of oscillatory flows in porous media, especially in systems where fluid viscosity varies under applied shear stress.

This paper explores the impact of mixed conduction, thermal radiation, rotation, and chemical reaction on the MHD flow of a viscous, incompressible, and electrically conductive fluid over a moving, inclined, heated porous plate. Numerical analysis techniques are strongly connected to perturbation theory. The original purpose of perturbation theory was to provide a solution to otherwise unsolvable issues with solar system planet motion calculations.

2 Mathematical Formulation

Consider a semi-infinite flow permeable plate immersed in a homogeneous porous medium susceptible to concentration and thermal with buoyancy effects and inclined at a vertical angle of α. The fluid being investigated is the viscosity, incompressible, heat-absorbing, and electrically charged fluid. The boundary layer is a laminar. For the wall, constant temperature T_ω and constant concentration C_ω over the surrounding ambient concentration C_∞ and temperature T_∞ respectively, are maintained. Furthermore, a first-order uniform chemical interaction with a rate constant R_a is postulated to exist between the distributing species and the fluid itself, taking into account the influence of rotation R. The governing equation of the fluid is influenced by this physical component. Based on the above presumptions, the basic equations characterizing the circumstances are stated on a linear frame of reference.

Continuity Equation:
$$\frac{\partial v}{\partial y} = 0 \implies v^* = -v_o \qquad (1)$$

Momentum Equation:
$$\rho v^* \frac{\partial u^*}{\partial y^*} = \mu \frac{\partial^2 u^*}{\partial y^{*2}} - \frac{\mu}{K} u^* - \sigma B_o^2 u^* + \rho g \beta_T (T^* - T_\infty) \cos\alpha + \rho g \beta_T (C^* - C_\infty) \cos\alpha + 2\Omega u^* \qquad (2)$$

Energy Equation:
$$\rho C_p v^* \frac{\partial T^*}{\partial y^*} = \alpha \frac{\partial^2 T^*}{\partial y^{*2}} + \mu \left(\frac{\partial u^*}{\partial y^*}\right)^2 - \frac{\partial q_r^2}{\partial y^*} + \sigma B_o^2 u^{*2} - Q_o (T^* - T_\infty) \qquad (3)$$

Concentration Equation:
$$v^* \frac{\partial C^*}{\partial y^*} = D \frac{\partial^2 C^*}{\partial y^{*2}} - R_a (C^* - C_\infty) \qquad (4)$$

The radiative flux of heat:
$$\frac{\partial q_r^*}{\partial y^*} = 4(T^* - T_\infty) I' \qquad (5)$$

where $I' = \int_0^\infty K_{\lambda\omega} \frac{\partial e_{b\lambda}}{\partial T^*} d\lambda$, $K_{\lambda\omega}$ is the wall's absorption coefficient and $e_{b\lambda}$ is Planck function.

The proper boundary conditions of the temperature, concentration, and velocity fields are derived as follows with these presumptions
$$u^* = 0, T^* = T_\infty, C^* = C_\infty \ at \ y = 0 \qquad (6)$$

$$u^* \to 0, T^* \to T_\infty, C^* \to C_\infty \ as \ y \to \infty \qquad (7)$$

The following non-dimensional variables are introduced
$$y = \frac{v_o y^*}{v}, \ u = \frac{u^*}{v_0}, \ M^2 = \frac{B_o^2 v^2 \sigma}{v_0^2 \mu}, K = \frac{K^* v_o^2}{v^2}, \ \rho = \frac{\mu}{v}, \theta = \frac{T^* - T_\omega}{T_\omega - T_\infty}, C = \frac{C^* - C_\omega}{C_\omega - C_\infty} \qquad (8)$$

The fundamental field equations (2)-(4) have a non-dimensional form that is
$$\frac{d^2 u}{dy^2} + \frac{du}{dy} - \left(M^2 - R + \frac{1}{K}\right) u = -Gr \cos\alpha - Gm \cos\alpha \qquad (9)$$

$$\frac{d^2 \theta}{dy^2} + Pr \frac{d\theta}{dy} + Pr \, Ec \left(\frac{du}{dy}\right)^2 - Pr(F + \phi) + Pr \, Ec M^2 u^2 = 0 \qquad (10)$$

$$\frac{d^2 C}{dy^2} + Sc \frac{dC}{dy} - Sc\gamma C = 0 \qquad (11)$$

In non-dimensional, the corresponding conditions for boundaries are:
$$u = 0, \theta = 1, C = 1 \ \ at \ y = 0 \qquad (12)$$

$$u \to 0, \theta \to 0, C \to 0, \ as \ y \to \infty \qquad (13)$$

3 Method of Solution

The equation (9)-(11) is a partial differential equation. This set of equations can be changed into a set of ordinary differential equations and solved analytically by taking the velocity u(y), temperature θ(y), and concentration C(y) in dimensionless form as follows:
$$u(y) = u_0(y) + Ec u_1(y) + O(Ec^2) \qquad (14)$$
$$\theta(y) = \theta_0(y) + Ec \theta_1(y) + O(Ec^2) \qquad (15)$$

$$C(y) = C_0(y) + Ec C_1(y) + O(Ec^2) \qquad (16)$$

when we solve for the zero-order coefficients of the Eckert number and omit the higher-order Eckert number $O(Ec^2)$, we obtain
$$u_o'' + u_o' - p u_o = -G_1 \theta_o - G_2 C_o \qquad (17)$$

$$\theta_o^{''} + \Pr\theta_o' + \Pr(F + \varphi)\theta_o = 0 \tag{18}$$

$$C_0^{''} + ScC_0' - Sc\gamma C_0 = 0 \tag{19}$$

when we solve for the first-order coefficients of the Eckert number, we obtain:

$$u_1^{''} + u_1' - pu_1 = -G_1\theta_1 - G_2C_1 \tag{20}$$

$$\theta_1^{''} + \theta_1' - \Pr(F + \varphi)\,\theta_1 + \Pr u_0'^2 + \Pr M^2 u_0^2 = 0 \tag{21}$$

$$C_1^{''} + ScC_1' - Sc\gamma C_1 = 0 \tag{22}$$

In this case, prime signifies regular distinction about "γ" and

$$p = \left(M^2 - R + \frac{1}{K}\right), G_1 = Gr\,cos\alpha, G_2 = Gm\,cos\alpha$$

The corresponding conditions for boundaries are:

$$u_0 = 0, u_1 = 0, \theta_0 = 0, \theta_1 = 0, C_0 = 0, C_1 = 0 \quad at\ y = 0 \tag{23}$$

$$u_0 \to 0, u_1 \to 0, \theta_0 \to 0, \theta_1 \to 0, C_0 \to 0, C_1 \to 0 \quad as\ y \to \infty \tag{24}$$

The following equation for concentration, temperature, and velocity is obtained by applying equations (23) and (24) to the equation (17)-(22).

$$u_0 = A_5(e^{-A_3y} - e^{-A_2y}) + A_6(e^{-A_3y} - e^{-m_2y}) \tag{25}$$

$$\theta_0 = e^{-A_2y} \tag{26}$$

$$C_0 = e^{-m_2y} \tag{27}$$

$$u_1 = B_{17}e^{-A_3y} - B_{10}e^{-A_2y} + B_{11}e^{-2A_2y} + B_{12}e^{-2A_3y} - B_{13}e^{-2A_{10}y} + B_{14}e^{-2m_2y} - B_{15}e^{-B_1y} + B_{16}e^{-B_2y} \tag{28}$$

$$\theta_1 = B_9e^{-A_2y} - B_3e^{-2A_2y} - B_4e^{-2A_3y} + B_5e^{-A_{10}y} - B_6e^{-2m_2y} + B_7e^{-B_1y} - B_8e^{-B_2y} \tag{29}$$

$$C_1 = 0 \tag{30}$$

Substituting equation (25)-(30) in equation (14)-(16), we get the final solution as follows:

$$u(y) = A_5(e^{-A_3y} - e^{-A_2y}) + A_6(e^{-A_3y} - e^{-m_2y}) + Ec\begin{pmatrix} B_{17}e^{-A_3y} - B_{10}e^{-A_2y} + B_{11}e^{-2A_2y} + B_{12}e^{-2A_3y} - \\ B_{13}e^{-2A_{10}y} + B_{14}e^{-2m_2y} - B_{15}e^{-B_1y} + B_{16}e^{-B_2y} \end{pmatrix} \tag{31}$$

$$\theta(y) = e^{-A_2y} + Ec(B_9e^{-A_2y} - B_3e^{-2A_2y} - B_4e^{-2A_3y} + B_5e^{-A_{10}y} - B_6e^{-2m_2y} + B_7e^{-B_1y} - B_8e^{-B_2y}) \tag{32}$$

$$C(y) = e^{-m_2y} \tag{33}$$

The wall shear stress τ_ω is provided by the physical parameters of interest:

$$\tau_\omega = \left(\mu\frac{\partial u^*}{\partial y^*}\right)_{y^*=0} = \rho v_0^2 u'(0)$$

The following provides the local skin friction factor

$$C_{fx} = \frac{\tau_\omega}{\rho v_0^2} = u'(0)$$
$$= A_6(m_2 - A_3) + A_5(A_2 - A_3) - Ec\begin{pmatrix} B_{17}A_3 - B_{10}A_2 + 2B_{11}A_2 + 2B_{12}A_3 \\ - B_{13}A_{10} + 2B_{14}m_2 - B_{15}B_1 + B_{16}B_2 \end{pmatrix} \tag{34}$$

The value of the local surface heat flux:

$$q_\omega = \left(-\kappa\frac{\partial T^*}{\partial y^*}\right)_{y^*=0}$$

Where the effective heat conductivity is denoted by κ

It is possible to express the local Nusselt number:
$$N_{u_x} = \frac{q_\omega}{(T_\omega - T_\infty)} \text{ as}$$

$$\frac{N_{u_x}}{R_{ex}} = \left(-\frac{\partial\theta}{\partial y}\right)_{y=0} \theta'(0) = A_2 + Ec(B_9A_2 - 2B_3A_2 - 2B_4A_3 + B_5A_{10} - 2B_6m_2 + B_7B_1 - B_8B_2) \tag{35}$$

The local surface mass flux is given by:

$$\frac{Sh_x}{R_{ex}} = \left(-\frac{\partial C}{\partial y}\right)_{y=0} = -m_2 \tag{36}$$

4 Results and Discussion

In Figure 1 we noticed that when the angle of inclination α increases, the velocity decreases. In this for distinct α the value of $Pr = 0.7, Sc = 0.6, M = 2.0, F = 3.0, \gamma = 0.1, Gr = 4.0, \alpha = 30^0, R = 3.0, \phi = 2.0, Gm = 2.0, E = 0.01$.

A fluid's flow properties are altered as the angle of inclination is increased when it flows along a surface that is inclined. A rise in the angle of inclination may result in a reduction in the fluid's velocity parallel to its surface for a particular flow rate. This is because a steeper inclination causes more gravitational force to operate against the direction of flow, which lowers the fluid's velocity over the surface. Figure 2 illustrates the Grashof number Gr on velocity distribution. Figure 2 shows

that velocity rises with increasing Grashof number. Higher Grashof values often result in greater fluid velocities. This is due to greater convective currents being driven by buoyancy forces, which become more dominating. Consequently, to accommodate the more violent motion caused by these forces, the fluid velocity rises.

Figure 3 illustrates how the magnetic parameter M affects velocity. This graphic shows that, when the plate cools, the velocity drops as the magnetic parameter increases. Particles with charge the fluid experience the intensity of Lorentz force of the magnetic field increases. This force prevents the fluid from moving, which increases flow resistance and lowers velocity. Figure 4 illustrates how the heat source parameter affects velocity. It is noticed that when the heat source ϕ rises, the velocity drops. The boundary layer of thermal energy close to the surface may thicken as ϕ rises. This larger boundary layer may make it more difficult for fluid to move near the surface, which decreases the fluid's total velocity.

Figure 5 shows how the velocity profile rises with increasing permeability parameter K. Higher permeability reduces the flow resistance in the medium, enabling the fluid to pass through it more quickly. The fluid's average velocity increases as a result. The fluid's velocity becomes more uniform, its average velocity rises and the pressure drop necessary for fluid flow falls as the permeability parameter K increases. Figure 6 shows that the velocity profiles rise in proportion to the modified Grashof number Gm. In general, a rise in the modified Grashof number Gm denotes a higher buoyancy effect than viscous forces inside the fluid. More vigorous movement of water is driven by higher buoyant forces. As a result, buoyancy forces strengthen the patterns of flow and improve convection movements overall, increasing fluid velocity.

Figure 7 illustrates how velocity drops as radiation parameter F's value rises. This is because of the decreased thermal buoyancy, the convection currents grow weaker and the velocity profiles become less noticeable. There might be a decrease in flow and an increase in laminar flow, which would result in a less varied and smaller velocity profile throughout the fluid, the improved radiative transmission of heat frequently lessens the importance of heat transfer by convection as the radiation parameter F rises, resulting in a drop in velocity.

Figure 8 shows the chemical reaction parameter rises, and velocity decreases. A velocity profile may decrease, and the chemical reaction rises as a result

of the process's effects on fluid dynamics and characteristics. This happens as a consequence of the reaction effects on fluid viscosity, density, and flow behavior as a whole, which frequently lead to a decrease in the intensity of convection currents and result in a drop in velocity. Figure 9 illustrates how the fluid velocity drops with increasing Schmidt number Sc. Larger momentum diffusivity, which causes the velocity to slow down, is indicated by a larger Schmidt number.

Figure 10 shows that the velocity profile decreases with increasing R. When rotational forces and fluid friction interact in rotating systems, the force of pressure distribution can get more complicated. Greater gradients in pressure caused by higher rotational rates have the potential to alter the velocity distribution and, as a result, frequently decrease the velocity in some systems. Figure 11 shows that when the Prandtl number Pr rises, velocity falls. A higher Prandtl number indicates that the fluid is more viscous, which increases flow resistance. The fluid's total velocity is lowered by this resistance. As a result, as the fluid gets more resistant to motion, its average velocity drops.

The temperature distribution graph in Figure 12 shows how it lowers as the heat source parameter ϕ increases. The temperature uniformity throughout the medium or layer can be enhanced by increasing the heat source parameter. This occurs as a result of the extra heat being dispersed more evenly, which causes reduced temperature. Figure 13 shows a graph showing how the temperature distribution drops as radiation parameter F increases. Because the radiative exchange of heat tends to smooth out variations in temperature more efficiently than conduction or convection alone, the relevance of temperature distribution reduces as the radiation parameter rises.

The consequences of raising the chemical reaction parameter γ and decreasing the concentration profile are shown in Figure 14. The rate at which reactants are transformed into products grows together with the chemical reaction variable. As a result, the concentration of reactants decreases more quickly and uniformly because they are consumed more quickly. As Schmidt number Sc levels increase, the concentration drops in Figure 15. In comparison to the kinematic viscosity, mass diffusivity is low if the Schmidt number is large. Because of their decreased mass diffusivity, the species become less likely to diffuse throughout the medium, which leads to less uniform concentration distributions. The slower diffusion mechanism makes the concentration gradients more important.

Ultimately, the various values of Sherwood number for various parameter values are shown in Figure 16. It illustrates the impact of $\in$ on Sherwood number Sh_x. It is noticed that with the rise of $\in$, Sherwood's number falls. Figure 17 shows the Nusselt number for various values of the aforementioned parameter n. Figure 17 shows how n affects the Nusselt number. It is noticed that the Nusselt number Nu_x rises with the n falls. Skin friction at various levels of Figure 18 allows for the aforementioned parameter for various values of $\in$. The impact of $\in$ on the skin friction C_{fx} is shown in Figure 18 in contrast to t. It has been noted that as $\in$ the skin friction rises as well.
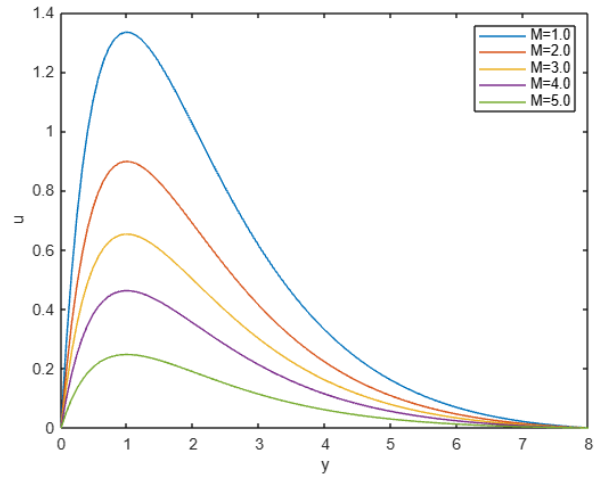
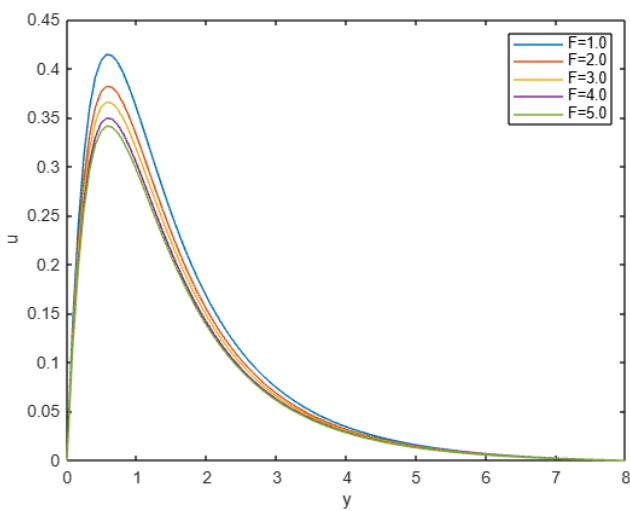
Fig. 3: Profile of velocity with distinct M
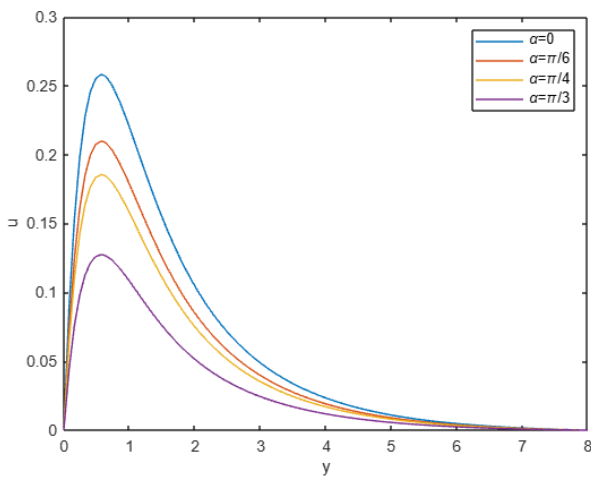
Fig. 1: Profile of velocity with distinct α
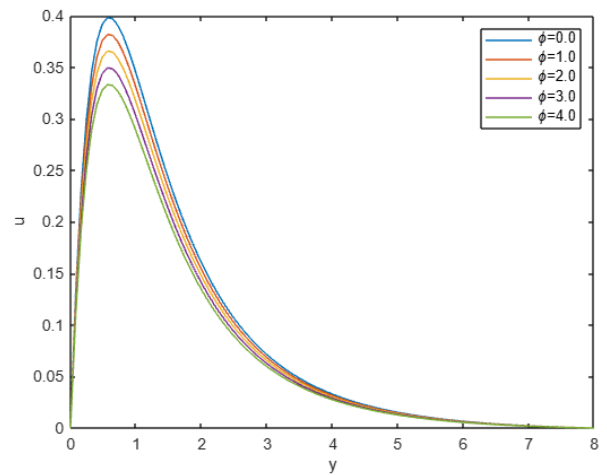
Fig. 4: Profile of velocity with distinct ϕ
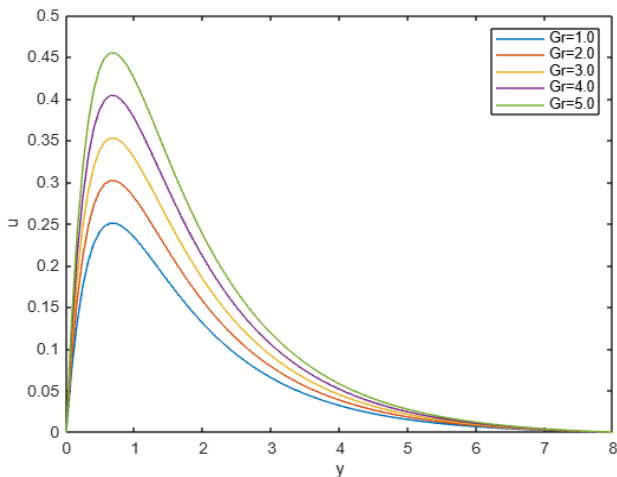
Fig. 2: Profile of velocity with distinct Gr
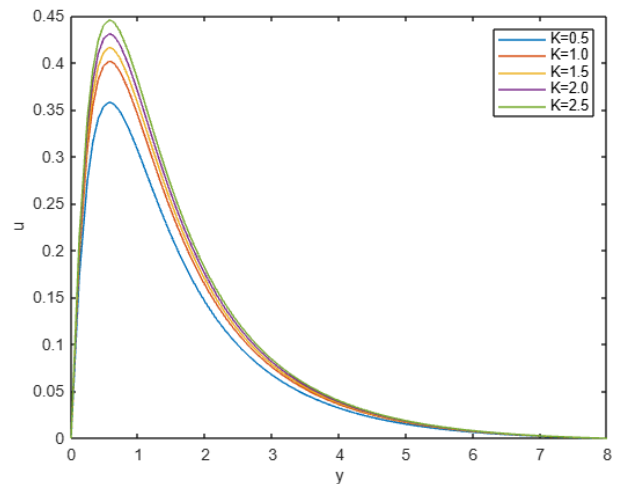
Fig. 5: Profile of velocity with distinct K
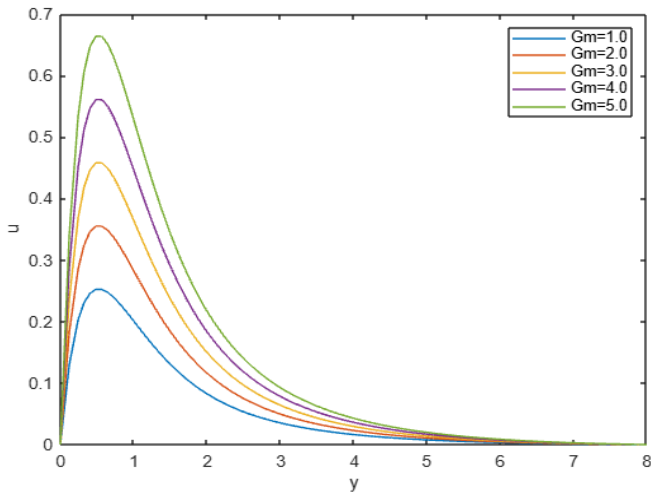
Fig. 6: Profile of velocity with distinct Gm
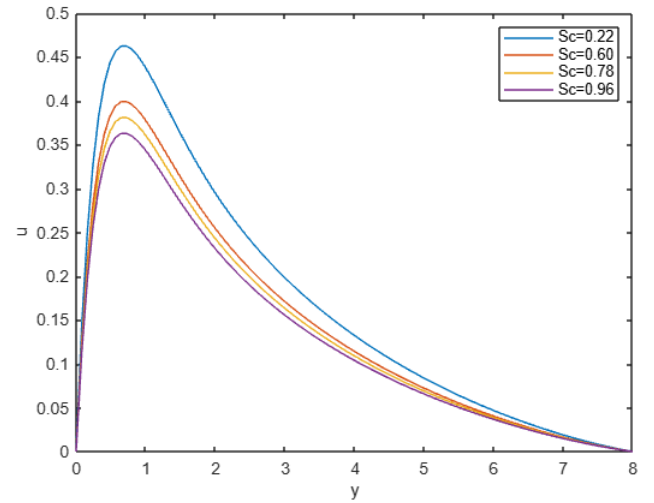
Fig. 9: Profile of velocity with distinct Sc

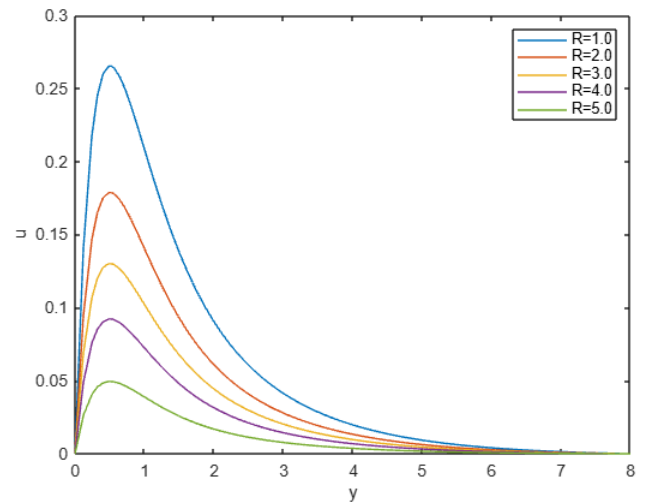Fig. 7: Profile of velocity with distinct F

Fig. 10: Profile of velocity with distinct R

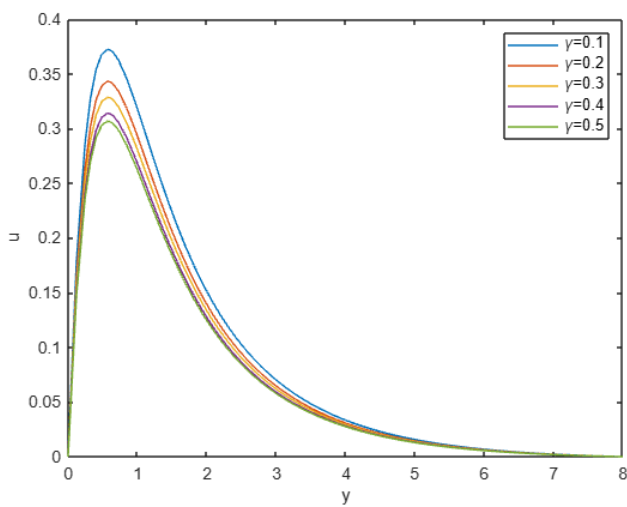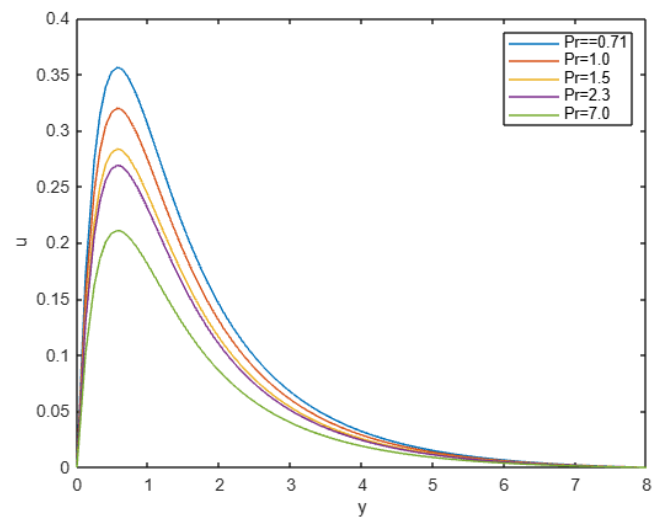

Fig. 8: Profile of velocity with distinct γ

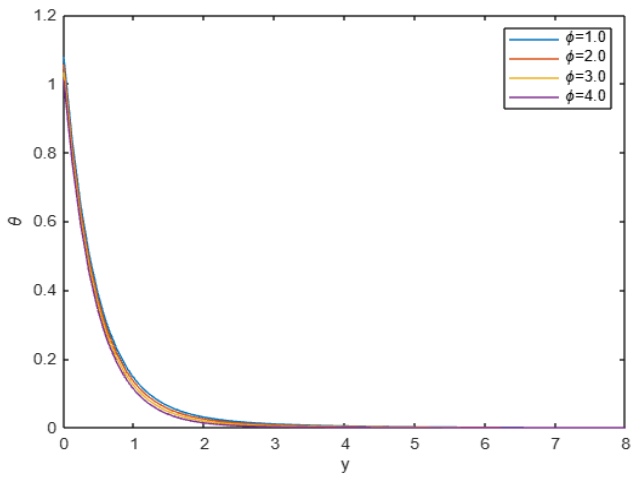Fig. 11: Profile of velocity with distinct Pr
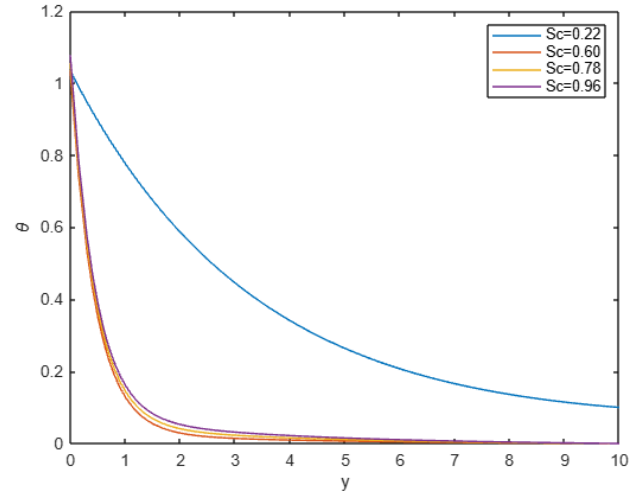
Fig.12:Profile of temperature with distinct ϕ
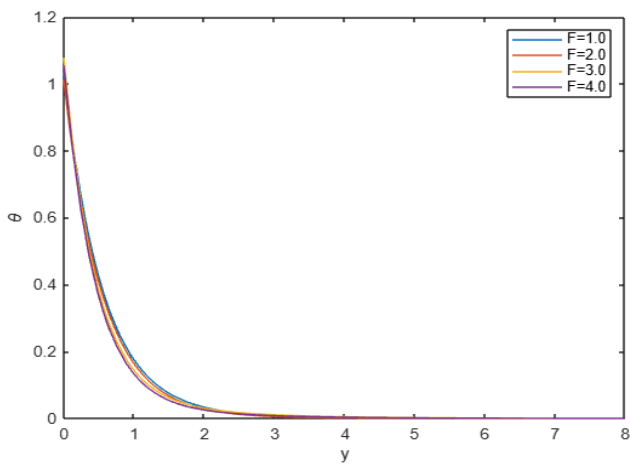

Fig. 15: Profile of concentration with distinct Sc

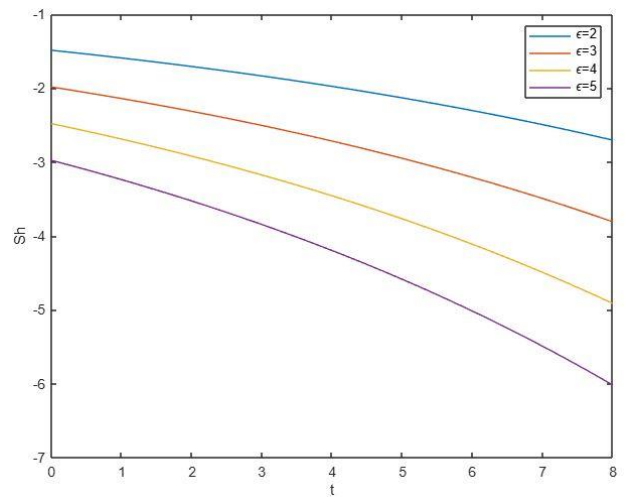Fig.13:Profile of temperature with distinct F
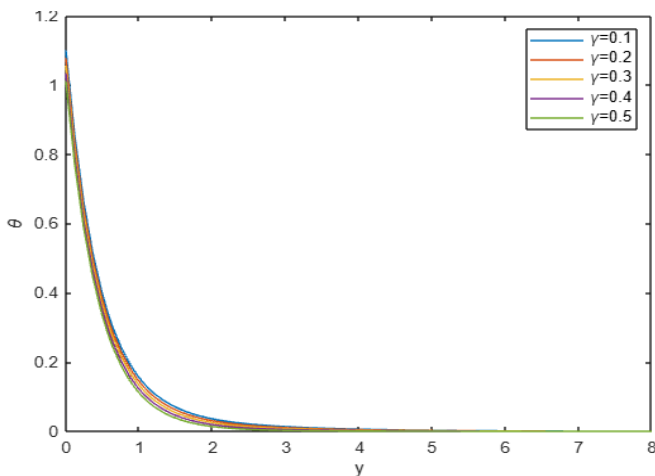

Fig. 16: Sherwood number for distinct values of ϵ versus t
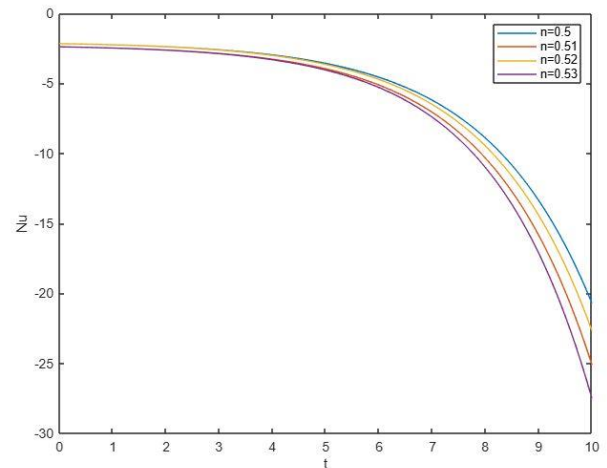

Fig. 14: Profile of concentration with distinct γ

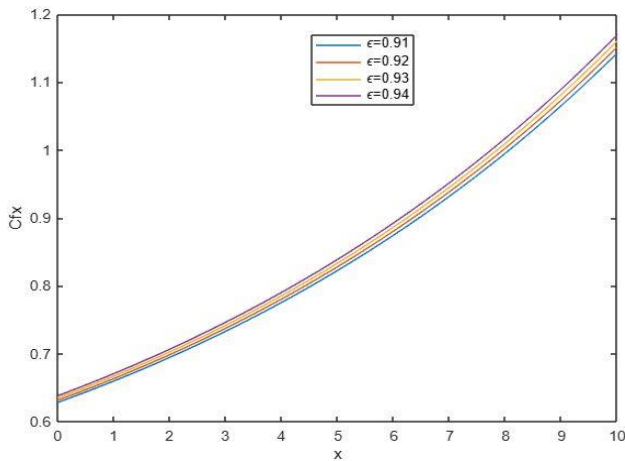Fig. 17: Nusselt number for distinct values of n against t

Fig. 18: Skin friction for distinct values of ϵ against t

5 Conclusion

The effects on the MHD flow of an incompressible, viscous, and electrically conducting fluid over a rotating inclined heated permeable plate with mixed convection combined with thermal radiation and a chemical reaction are examined. The linked partial differential equations that are non-linear include resolved using the perturbation approach. The impact of several relevant temperature, velocity, and concentration distribution characteristics has been examined and evaluated using graphs. In this investigation, the following results are made.

1. Increases in the angle of inclination (α), radiation, chemical reaction, heat source parameter, Rotational, and Schmidt number Sc cause the velocity to decrease; in contrast the modified Grashof number(Gm), Grashof number (Gr), and permeability parameter (K) cause the velocity to show a reverse tendency.
2. As heat source (ϕ) and radiation parameter (F) rise, the temperature distribution falls.
3. The concentration boundary layer drops as the Schmidt number (Sc) and chemical reaction parameter (γ) rise.

Declaration of Generative AI and AI-assisted Technologies in the Writing Process
The authors wrote, reviewed and edited the content as needed and they have not utilized artificial intelligence (AI) tools. The authors take full responsibility for the content of the publication.

References:
[1] Areekara S, Sabu AS, Mathew A, Oke AS. "Transport phenomena in Darcy-Forchheimer flow over a rotating disk with magnetic field and multiple slip effects: modified Buongiorno nanofluid model", *Waves Random Complex Media*, 2023, 1-20. 10.1080/17455030.2023.2198611.
[2] Oke AS., "Heat and mass transfer in 3D MHD flow of EG-based ternary hybrid nanofluid over a rotating surface", *Arab J Sci Eng*, 47(12), 2022, 16015-31.
[3] Samuel OA, "Coriolis effects on air, nanofluid, and Casson fluid flow over a surface with nonuniform thickness". ([doctoral dissertation], 2022, (Kenyatta University).
[4] Choudhury K, Ahmed N., "Unsteady MHD mass transfer flow past a temporarily accelerated semi-infinite vertical plate in the presence of thermal diffusion with ramped wall temperature", *Math. Model. Eng. Problem*, 6(2), 2019, 241-248.
[5] Srinathuni Lavanya, Devika B, Chenna Kesavaiah D., "Radiation effect on unsteady free convective MHD flow of a viscoelastic fluid past a tilted porous plate with heat source", *Journal of Xidian University*, Vol. XII (V), 2020, 525-543.
[6] Raju M, Venkateswara Raju K, Chandra Reddy P, Changal Raju M, Sankara Sekhar Raju G., "Heat generation and chemical reaction impact on MHD rotating flow past a vertical porous plate", *Turkish Journal of Computer and Mathematics Education*, Vol.12 (13), 2021, 3101-3111.
[7] Kumar D, Singh AK, Kumar D., "Influence of heat source/sink on MHD flow between vertical alternate conducting walls with Hall effect", *Physica A*, Vol. 544, 2020, 123562.
[8] Raghunath K, Mohanaramana R., "Hall, Soret and rotational effects on unsteady MHD rotating flow of a second-grade fluid through a porous medium in the presence of chemical reaction and aligned magnetic field", *Int. Commun. Heat Mass Transf.*, 137, 2022, 106287.
[9] Muthucaraswamy R., "Effects of a chemical reaction on a moving isothermal vertical surface with suction", *Acta Mech*, 155, 2002, 65-70.
[10] Juma BA, Oke AS, Mutuku WN, Ariwayo AG, Ouru OJ., "Dynamics of Williamson fluid over an inclined surface subject to Coriolis and Lorentz forces", *J Eng Appl Sci*, 5(1), 2022, 37-46.

R. Kavitha, J. Angel

[11] Waqas H, Sami Ullah Khan, Bhatti MM, Imran M., "Significance bioconvection in the chemical reactive flow of magnetized Carreau–Yasuda nanofluid with thermal radiation and second-order slip", *Journal of Thermal Analysis and Calorimetry*, 140, 2020, 1293-1306.

[12] Ganie AH, Mah MM, AlBaidani Z, Alharthi NS, Khan U., "Unsteady non-axisymmetric MHD Homann stagnation point flow of CNTs-suspended nanofluid over the convective surface with radiation using Yamada–Ota model", *Int. J. Mod. Phys. B*, 2023, 2350320.

[13] Mahmood Z, Abd El-Rahman M, Khan U, Hassan AM, Khalifa HAE-W., "Entropy generation due to nanofluid flow in porous media over radiative permeable exponentially surface with nanoparticle aggregation effect", *Tribol. Int.*, 188, 2023. 108852.

[14] Reddy SC, Asogwa KK, Yassen MF, Iqbal Z, Ali B, Km S., "Dynamics of MHD second-grade nanofluid flow with activation energy across a curved stretching surface", *Front. Energy Res.*, 10, 2022, 1007159.

[15] Rafique. K, Z. Mahmood, U. Khan., "Mathematical analysis of MHD hybrid Nanofluid flow with variable viscosity and slip conditions over a stretching surface", *Mater. Today Commun.* 36, 2023, 106692.

[16] Yashkun U, Zaimi K, Ishak A, Pop I, Sidaoui R., "Hybrid nanofluid flow through an exponentially stretching/shrinking sheet with mixed convection and Joule heating", *Int. J. Numer. Methods Heat Fluid Flow*, 31 (6), 2021, 1930-1950.

[17] Patil PM, Goudar B., "Impact of impulsive motion on the Eyring-Powell nanofluid flow across a rotating sphere in MHD convective regime: entropy analysis", *J. Magn. Magn Mater.*, 571, 2023, 170590.

[18] Patil PM, Benawadi S, Shanker B., "Influence of mixed convection nanofluid flow over a rotating sphere in the presence of diffusion of liquid hydrogen and ammonia", *Math. Comput. Simulat.*, 194, 2022, 764–781.

[19] Raghunath K, Nagesh G, Reddy VRC, Obulesu M., "Unsteady MHD fluid flow past an inclined vertical porous plate in the presence of chemical reaction with aligned magnetic field, radiation, and Soret effects", *Heat Transf.*, 51, 2021, 2742–2760.

[20] Ali B, Ahammad NA, Windarto, Oke AS, Shah NA, Chung JD, J. D., "Significance of tiny particles of dust and TiO2 sub ject to Lorentz force: The case of a non-Newtonian dusty rotating fluid", *Mathematics*, 11(4), 2023, 877.

[21] Raghunath K, Obulesu M., "Unsteady MHD oscillatory Casson fluid flow past an inclined vertical porous plate in the presence of chemical reaction with heat absorption and Soret effects", *Heat Transf.*, 51, 2022, 733–752.

Contribution of Individual Authors to the Creation of a Scientific Article (Ghostwriting Policy)

Sources of Funding for Research Presented in a Scientific Article or Scientific Article Itself

Conflict of Interest

The authors have no conflicts of interest to declare

Creative Commons Attribution License 4.0 (Attribution 4.0 International, CC BY 4.0)

APPENDIX

$$Gr = \frac{\rho g \beta_T v^2 (T_\omega - T_\infty)}{v_0^3 \mu},$$

$$Gm = \frac{\rho g \beta_c v^2 (C_\omega - C_\infty)}{v_0^3 \mu},$$

$$Pr = \frac{\mu C_p}{\alpha},$$

$$\gamma = \frac{R_a v}{v_0^2},$$

$$Ec = \frac{v_0^2}{C_p (T_\omega - T_\infty)},$$

$$F = \frac{4vI'}{\rho C_{p v_0^2}},$$

$$\varphi = \frac{Q_0 v}{\rho C_{p v_0^2}},$$

$$Sc = \frac{\gamma}{D},$$

$$R = \frac{2\Omega M^2}{B_0^2 \sigma}$$

$$R_{e_x} = \frac{v_0 x}{v}$$

$$m_2 = \frac{Sc + \sqrt{Sc^2 + 4Sc\gamma}}{2},$$

$$A_2 = \frac{Pr + \sqrt{Pr^2 + 4Pr(F+\phi)}}{2},$$

$$A_3 = \frac{1 + \sqrt{1+4p}}{2}, A_5 = \frac{G_1}{A_2{}^2 - A_2 - p},$$

$$A_6 = \frac{G_2}{m_2{}^2 - m_2 - p},$$

$$A_{10} = A_2 + A_3, A_{11} = A_5 + A_6,$$

$$B_1 = A_3 + m_2,$$

$$B_2 = A_2 + m_2,$$

$$B_3 = \frac{Pr A_5{}^2 (A_2{}^2 + M^2)}{4A_2{}^2 - 2Pr A_2 - Pr(F+\phi)},$$

$$B_4 = \frac{Pr A_{11}{}^2 (A_4{}^2 + M^2)}{4A_3{}^2 - 2Pr A_3 - Pr(F+\phi)},$$

$$B_5 = \frac{2Pr A_5 A_{11} (A_2 A_3 + M^2)}{A_{10}{}^2 - Pr A_{10} - Pr(F+\phi)},$$

$$B_6 = \frac{Pr A_6{}^2 (m_2{}^2 + M^2)}{4m_2{}^2 - 2Pr m_2 - Pr(F+\Phi)},$$

$$B_7 = \frac{2Pr A_{11} A_6 (A_3 m_2 + M^2)}{B_1{}^2 - Pr B_1 - Pr(F+\phi)},$$

$$B_8 = \frac{2Pr A_5 A_6 (A_2 m_2 + M^2)}{B_2{}^2 - Pr B_2 - Pr(F+\phi)},$$

$$B_9 = B_3 + B_4 - B_5 + B_6 - B_7 + B_8,$$

$$B_{10} = \frac{G_1 B_9}{A_2{}^2 - A_2 - P}, \ B_{11} = \frac{G_1 B_3}{4A_2{}^2 - A_2 - P},$$

$$B_{12} = \frac{G_1 B_4}{4A_3{}^2 - A_3 - P}, \ B_{13} = \frac{G_1 B_5}{A_{10}{}^2 - A_{10} - P},$$

$$B_{14} = \frac{G_1 B_6}{4m_2{}^2 - m_2 - P}, B_{15} = \frac{G_1 B_7}{B_1{}^2 - B_1 - P},$$

$$B_{16} = \frac{G_1 B_8}{B_2{}^2 - B_2 - P},$$

$$B_{17} = B_{10} + B_{13} + B_{15} - B_{11} - B_{12} - B_{14} - B_{16}$$